Spontaneous Raman scattering for simultaneous measurements of in-cylinder species

Spontaneous raman scattering for simultaneous measurements of in-cylinder species

H Zhao and S Zhang
School of Engineering and Design, Brunel University, Uxbridge, UB8 3PH, UK

Abstract: A technique for multi-species mole fraction measurement in internal combustion engines is described. The technique is based on the spontaneous Raman scattering. It can simultaneously provide the mole fractions of several species of N_2, O_2, H_2O, CO_2 and fuel. Using the system, simultaneous measurement of air/fuel ratio and burnt residual gas are carried out during the mixture process in a Controlled Auto Ignition (CAI) combustion engine. The accuracy and consistency of the measured results were confirmed by the measured air fuel ratio using an exhaust gas analyzer and independently calculated mole fraction values. Measurement of species mole fractions during combustion process has also been demonstrated. It shows that the SRS can provide valuable data on this process in a CAI combustion engine.

Introduction

Controlled Auto Ignition (CAI) combustion, also known as Homogeneous Charge Compression Ignition (HCCI), has emerged as a viable alternative combustion process to the conventional SI or Compression Ignition (CI) process because of its potential for high efficiency and extremely low emissions of nitrogen oxide and particulate emissions. One of the difficulties for the application of CAI combustion to normal gasoline engines is for the cylinder charge to reach sufficiently high temperature for auto-ignition. Mixing the hot residual gas with fresh charge has presented as a promising approach to increase the charge temperature, high enough to initiate the auto-ignition. It has been shown that the distribution of residual gas or stratified residual gas could influence the auto-ignition and the subsequent combustion process [1]. In order to study the effect of residual gas and the charge stratification on their combustion process, it is important to be able to measure the air/fuel ratio and the residual gas in the CAI combustion engines**.**

Planar Laser Induced Fluorescence (PLIF) was used previously and it provided useful information of the fuel concentration distribution in the cylinder of a CAI engine [1, 2]. However, the PLIF technique is limited to qualitative measurement of fuel distribution. In order to understand the effect of mixture composition and species distribution on the combustion process, simultaneous and quantitative measurements of multiple species are needed. This can be realised by the Spontaneous Raman Scattering (SRS) measurement.

The application of SRS for in-cylinder multiple species measurement was first implemented by Johnson [3, 4]. Using a gated CW laser Raman system, the author measured the air fuel ratio distribution and studied the stratification combustion process in a SI engine. Some recent examples for the application of SRS with 248.62nm KrF Excimer laser to mixture formation analysis in SI engines are given in references [5-8]. The measurement of all the major species in SI engines with a SRS system based on a 532nm Nd:YAG laser are presented in references [9-11].

In this work, a SRS system based on a 532nm Nd:YAG laser and its measurement of all the major species in a CAI combustion engine is present.

Principle

Raman scattering is the radiation of the incident photons lost their energies to or gained energies from the molecular vibrational, or rotational energies as a result of inelastic collisions between the photons and molecules. The radiation of photons lost and holding lower energies gives rise to Stokes Raman scattering, and conversely, the radiation of photons gained and holding higher energies gives rise to anti-Stokes Raman

scattering. Since the probability of photons lost their energies to molecules is normally much higher than gained energies from molecules, the anti-Stokes scattering is much weaker than the Stokes scattering.

The process of Raman scattering is illustrated in Figure 3.1. It can be visualized as the absorption of incident photon energy by a molecule of a given initial state, raising the molecule to a "virtual" state, from which it immediately returns to a final stationary state emitting a photon with different energy. The energy of the emitted photon can be given by the incident photon energy pluses the energy difference between the initial state and the final state of the molecule.
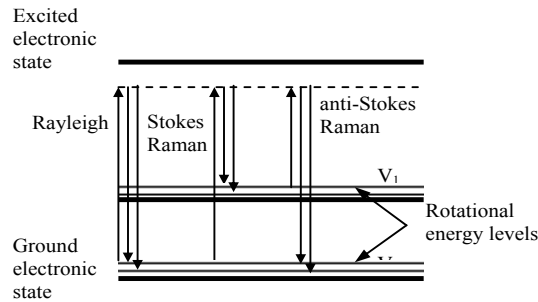

Figure 1 Schematic of an energy diagram for
Rayleigh and Raman scattering

Raman scattering energy from species i, scattered into a solid angle Ω, is usually expressed in terms of the differential scattering cross section $(\partial\sigma/\partial\Omega)_i$

$$E_i = \eta E_0 N_i \Omega l_C \left(\frac{\partial\sigma}{\partial\Omega}\right)_i \quad (1)$$

where E_0 is the incident laser energy; η is the delivery efficiency, N_i is the number density of molecular species i. In general, a SRS system for the measurement of gas concentration is based on the detection of Stokes vibrational Raman scattering. For diatomic molecules, the Stokes Raman scattering cross-section can be expressed as

$$\left(\frac{\partial\sigma}{\partial\Omega}\right) = \varepsilon N_i f(T) \frac{(\tilde{v}_0 - \Delta\tilde{v})^4}{\Delta\tilde{v}} \quad (2)$$

where ε is a constant; $\tilde{v}_0$ is the wavenumber of incident laser; $\Delta\tilde{v}$ is the wavenumber of Raman shift; and $f(T)$ describes the temperature dependency of the Raman scattering cross section and is given as

$$f(T) = \frac{1}{1 - \exp(-h\tilde{v}_e/2\pi KT)} \quad (3)$$

where h is the Planck's constant, K is the Boltzmann's constant and T is the absolute temperature.

Equations (2) and (3) indicate that the temperature imparts a positive effect. The higher the gas temperature is, the larger the Raman scattering cross-section becomes. For polyatomic molecules, more complex expressions for the scattering cross-section arise, but the conclusion drawn from Equations (2) and (3) regarding the temperature dependence of the cross-section is still valid.

In practice, the species concentration is measured from the Raman scattering signal in some spectral integrated portion of the Raman scattering. According to Equations (1), (2) and (3), the Raman scattering signal strength of species i can be given as:

$$S_i = k_i E_0 N_i \quad (4)$$

where k_i is a factor dependent on the Raman cross-section, the incident laser wavenumber, the geometric optical collection efficiency, the gas temperature and the spectrally region which is selected for the integration. After

determining k_i by calibration from Raman scattering in a known sample by independent measurements, the species concentration N_i can be calculated from the measured Raman scattering from Equation (4).

Normally, if the gas temperature is much lower than the characteristic vibrational temperature of the species to be measured, given by $T_V=hc\omega_e/k$, where the grouping hc/k have a value of $1.44 Kcm^{-1}$, the temperature effect can be ignored. In this case, k_i is a constant. However, when the temperature is higher than or comparable to the characteristic vibrational temperature, the temperature effect needs to be considered.

Experiment

The measurement was performed in a single cylinder optical research engine at Brunel University. Details of the engine are given in Table 1.

Table 1 Details of the single cylinder engine

Bore	95.3mm
Stroke	89mm
Compression Ratio	10:1
Intake Valve Opening	20 ATDC
Intake Valve Closure	40 ABDC
Exhaust Valve Opening	BDC
Exhaust Valve Closure	20 ATDC
Valve diameter	19mm
Valve lift	4mm

The engine has a disk-shaped combustion chamber with a flat fused silica window on the top, which permits a complete view of the combustion chamber, as shown in Figure 2. There are also two side windows that allow the transmission of a laser beam or a laser sheet, so that a laser diagnostic technique can be applied for the measurement of mixture distribution in the combustion chamber. The ingenious part of the engine design is the specially arranged intake and exhaust valves, as shown in Figure 3. The two intake valves are positioned so that the cylinder wall shrouds their outer edges. Hence, two concentric flows may be formed in the combustion chamber. The two inlet streams can be of identical air-fuel mixtures which can give a relatively uniformly mixture distribution in the cylinder. Or by having the different air/fuel ratios in the two ports, a stratified charge may be formed. A greater degree of charge stratification can be achieved if one of the intake ports is used to admit only air or EGR.

The experimental set-up is shown in Figure 4. A 532nm Nd:YAG pulsed laser was selected as the laser source. The polarization plane of the laser beam was set to be perpendicular to the scattering plane. A laser pulse stretcher was employed to extend the laser pulse duration. The laser beam was then focused at the centre of the combustion chamber by a focusing lens and delivered into the engine at about 3mm below the bottom surface of the top window, which is about one-half of the engine clearance height. Scattered light was observed from the top of the engine, but its travelling direction was changed 90° by a mirror. The scattered light was then focused by a pair of achromatic lenses onto the entrance slit of a spectrometer. To block the Raleigh scattering and other spurious light from reaching the detector, a holographic notch filter is placed in the front of the entrance slit of the spectrometer. The spectrometer output was detected by an ICCD camera, in which the Raman spectra of the measured species were recorded.
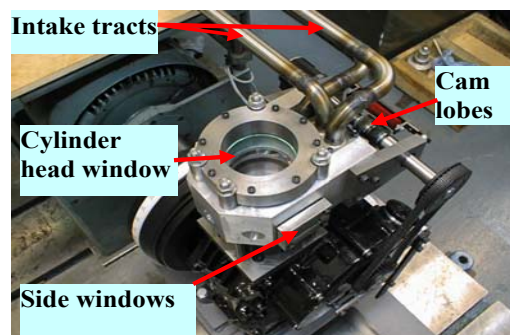

Figure 2 Photograph of the single cylinder optical engine
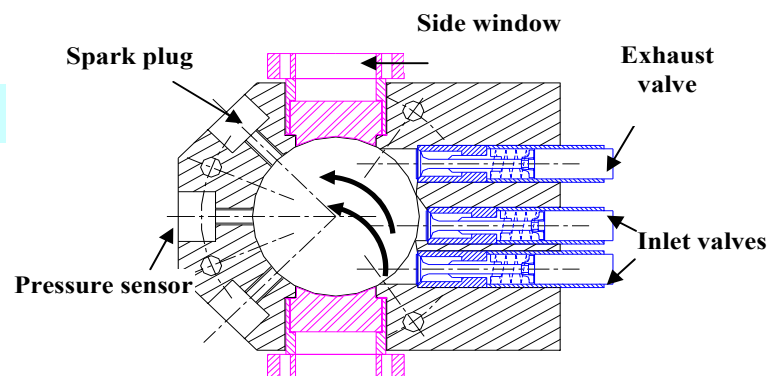

Figure 3 Schematic of the cylinder head design

The pulse stretcher operated by splitting off a portion of the beam and passing it through an optical delay loop before recombining it with the original beam. As a result, the duration of laser pulses was expanded and intensity peak of each pulse decreases. A schematic representation of the temporal intensity profile of a laser pulse before and after passing through the pulse stretcher is shown in Figure 5. By employing the pulse stretcher, the laser energy that could be delivered to the test section with each pulse was increased about 4 times without breaking the access windows or causing the gas broken down to occur.
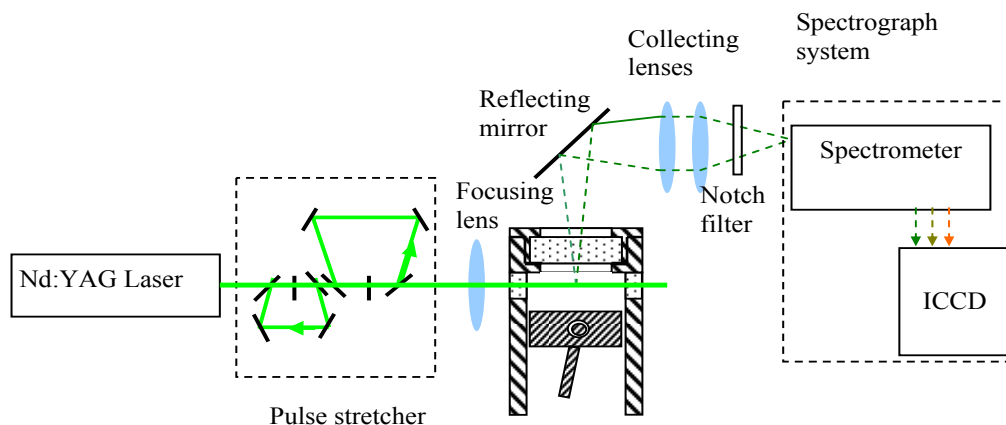
.

Figure 4 Optical set-up of the SRS system

Figure 5 Temporal intensity profile of the laser before and after pulse stretch.

A spherical lens with 300mm focal lens was employed as the focusing lens, with which the focused beam waist of 102μm in diameter and distances of 7.6mm on either side of the waist before the beam diameter doubled were formed in the test section. The scattered light was collected by two identical achromatic lenses with a focal length of 310mm and clear optical aperture of 78mm. The collecting lenses gave F-numbers of 3.97 (=310/78), which was chosen to be close to the F-number of 3.8 of the spectrometer for a high-collection efficiency.

 600 mm^{-1} grating was used to spectrally disperse the collected light by about 12.6nm/mm in the plane of the detector. With a 20.8mm CCD detector array width, this provided approximately 262nm-wavelength coverage. This was sufficient to simultaneously monitor all of the major species of combustion.

The engine was motored at a speed of 600 rpm. iso-octane/n-heptane (40:60 in volume) was used as the fuel. Two identical air fuel mixtures were used, so that a relatively uniform-mixture distribution were formed in the cylinder. In order to attain the controlled auto-ignition, the intake air was heated to 100°C and the relative

air/fuel ratio was set to 1.6. A richer mixture than $\lambda=1.6$ led to rapid heat release and knocking-like violent combustion. A leaner mixture than $\lambda=1.6$ caused the engine to fire intermittently.

Data interpretation and system calibration

Several species, mainly O_2, N_2, H_2O, CO_2 and fuel, are present in the cylinder of IC engines before and during the combustion. As far as the spectrum of Stokes vibrational-rotational Raman scattering of the mixture is considered, it includes several spectral peaks. For each species, there may be one or more spectral peaks. For example, most fuels used in IC engines may have several Raman spectral peaks, which result from different vibrational-rotational modes. However, normally, for the measurement of concentration, only one peak, is considered. Figure 6 gives a schematic representation of the Raman spectrum, O_2, N_2, H_2O, CO_2 and fuel mixture. There are three Raman spectral modes, CH, CC and CH_3 associated with the fuel and two modes, v_1 and $2v_2$, associated with CO_2. As fuel CH mode has the strongest signal peak, it is chosen for the measurement of the fuel concentration. As the CO_2 $2v_2$ peak is interfered by the fuel CH_3 and the O_2 peaks, CO_2 v_1 peak is selected for the concentration acquisition of CO_2 though its peak intensity is slight lower than that of the CO_2 $2v_2$ peak. The signal strength of O_2 is acquired by subtracting the signal strength of the CO_2 $2v_2$ peak and the fuel CH_3 peak from the total signal strength over the three overlapped peaks (CO_2 $2v_2$ peak + fuel CH_3 peak + O_2 peak). According to the principle of Raman scattering, the ratio between the signal strengths of two certain regions of a species should remain constant. Therefore, the signal strengths of CO_2 $2v_2$ peak and the C_3H_8 CH_3 peak can be determined from the signal strengths of the CO_2 v_1 peak and the C_3H_8 CH peak. The ratios between the signal strengths of the two peaks of CO_2 and the two peaks of fuel can be determined by calibration.
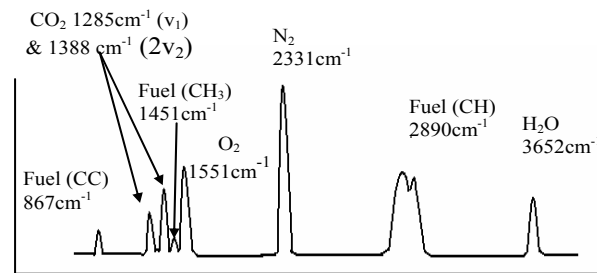

Figure 6 Schematic representation of the Raman spectrum
of a mixture of N_2, O_2, H_2O, CO_2 and fuel

As shown in Equation (4), the concentration of each species in the mixture can be obtained from the signal strengths after the calibration factor, k_i, and the delivery laser energy in the measurement volume has been determined. However, the result will be affected by pulse to pulse laser variation or altered by the window fouling

In this experiment the mole fraction was determined instead, which can be obtained by the following equation:

$$\chi_i = \frac{N_i}{\sum\limits_i N_i} = \frac{S_i/E_0 k_i}{\sum\limits_i S_i/E_0 K_i} = \frac{\dfrac{S_i}{S_{N_2}}\Big/\dfrac{K_i}{K_{N_2}}}{\sum\limits_i \left(\dfrac{S_i}{S_{N_2}}\Big/\dfrac{K_i}{K_{N_2}}\right)} \qquad (5)$$

Equation (5) shows that the mole fraction is dependant on the signal strength of a species relative to that of N_2, S_i/S_{N_2}, and a system response-factor relative to that of N_2, K_i/K_{N_2}. As both the S_i/S_{N_2} and the K_i/K_{N_2} are independent on the incident laser energy, errors due to variation in the incident laser energy by the pulse to pulse variation in the laser output and widow fouling are obliterated.

Calibration of K_i/K_{N_2} corresponding species i is performed by putting it together with N_2 in a calibration cell at a known temperature. The result is given in Table 2.

From the data given in Table 2, the ratios between the signal strength of the two peaks of CO_2 and the two peaks of fuel can be obtained and are given as 1.2179 and 0.064419, respectively.

Table 2 Calibration factors relative to of the species N_2

Species	Peak position (nm)	Temperature (K)	Calibration factor
O_2	579.8	313	1.5411
CO_2	571.0	313	1.2000
	574.4	313	1.4615
Fuel	628.6	313	25.820
	576.5	313	1.6633
H_2O	660.3	453	2.0412

It should be noted that the calibration factors given in Table 2 could only be used when in-cylinder temperature was much lower than the characteristic vibrational temperature of the species to be measured. However, the gas temperature in the cylinder could be very high at the later stage (about 1050K) of the compression stroke, particularly, after auto-ignition started (more than 1050K), It was necessary to consider the effect of temperature on the measurement. As limited by the length of this paper, Further details on how to correct the measurement error owning to temperature effect will not be present. In the discussion below, when the mole fraction of species are calculated, the effect of temperature has been considered.

The residual gas mole fractions can be independently found from the measured mole fraction of each species based on lean burn combustion reaction of iso-octane/n-heptane (40:60 in volume) at a relative air/fuel ratio of λ

$$\chi_r = \frac{53.544\lambda + 3.872}{7.372}\chi_{CO_2} \qquad (6)$$

$$\chi_r = \frac{53.544\lambda + 3.872}{7.744}\chi_{H_2O} \qquad (7)$$

$$\chi_r = 1 - (53.544\lambda + 1)\chi_{fuel} \qquad (8)$$

$$\chi_r = \lambda \frac{53.544\lambda + 3.872}{56.461\lambda + 1} \times \left(1 - \frac{53.544\lambda + 1}{11.244\lambda}\chi_{O_2}\right) \qquad (9)$$

From the measured fuel and O_2 mole fractions, the relative air/fuel ratio could be calculated as given by

$$\lambda = \frac{\chi_{O_2}}{11.244\chi_f} \qquad (10)$$

Results and Discussion

Ensemble-averaged (200 cycles) Raman spectra were recorded in the operating engine at various crank angles from the beginning of intake stroke to the end of the in-cylinder combustion at about 15°CA ATDC at the expansion stroke. Sample spectra are shown in Figure7.

As discussed above, the signal strengths associated with the species were obtained by integrating over appropriated spectral regions. Since the spectral peaks were polluted by random noise and superimposed on a baseline, prior to integration, the baselines were found by polynomial fittings and removed by subtracting it from the original spectrum. In addition, the random noises were minimized by a five point smoothing method.

After signal strengths were obtained, the mole fractions of species were calculated by using Equation (5). The measured mole fractions of O_2, fuel, H_2O and CO_2 as a function of crank angle (after considering the effect of temperature on the measurement result) are given in Figure 8. It can be seen that only residual gases were present in the chamber from -350°CA ATDC until -300°CA ATDC. The air (O_2) and fuel started to appear at -290°CA ATDC and their mole fractions kept increasing to reach a local maximum value at about -280°CA ATDC. These variation in their values indicated that, the air, fuel and residual gas were not thorough mixed from -280°CA ATDC until to approximately -120 °CA ATDC. The mole fractions of the species stayed approximately constant from about -120°CA ATDC until -20°CA ATDC. Between -20°CA ATDC to TDC the mole fractions of fuel and O_2 slowly decreased whereas the mole fractions of H_2O and CO_2 slowly increased, indicating that ignition was started during this period of time. After TDC the mole fractions of fuel and O_2

dropped rapidly while the mole fraction of H_2O and CO_2 rose rapidly, indicating that the main combustion was taking place during this period of time.

Figure 9 shows the calculated residual gas fractions based on the measured mole fraction of each species. Overall, the calculated results agreed well with each other. The noticeable discrepancy between CO_2 and the rest was probably due to the relative weak SRS signal and error induced in the peak area measurement. The anomaly in the fuel based results near 280°CA BTDC was possibly due to the stratification present in the early intake stroke. The results shown in Figure 9 were consistent with the fact that the cylinder was filled with burned gases (about 100% residual fraction) before the inlet valves were open. The concentration of burned gases remained constant during the compression stroke before it reached another peak after the combustion had started.

Figure 10 shows the relative air/fuel ratio obtained from the measured fuel and O_2 by using Equation (9). It can be seen that the measured in-cylinder relative air/fuel ratio was about, very close to the value of 1.6 measured by an exhaust gas analyser confirming the SRS measurement was correct.
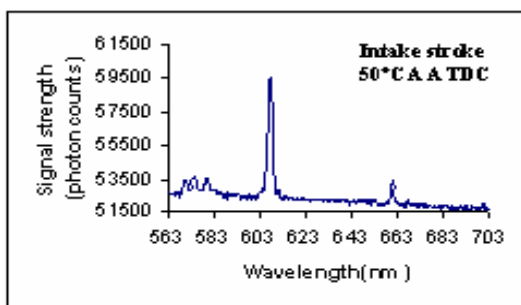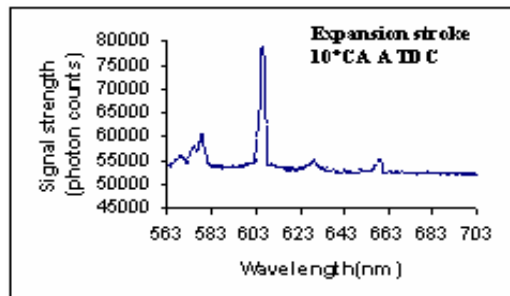

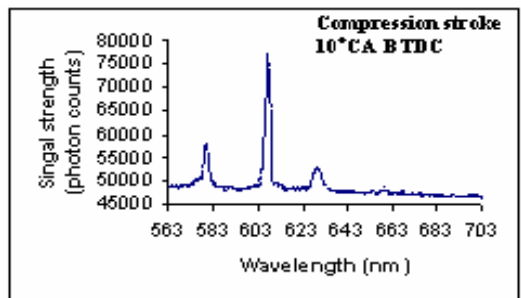(a) SRS spectrum just before the first appearance of fuel
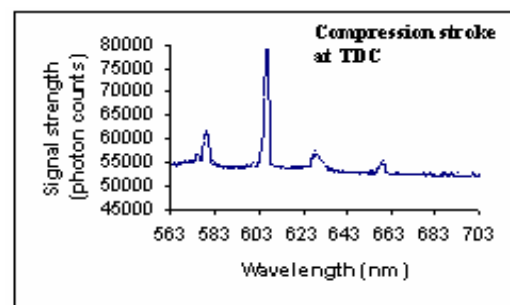
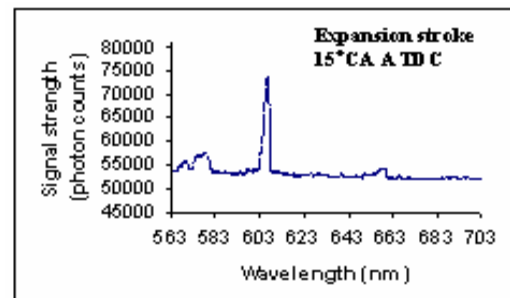(d) SRS spectrum at the start of combustion
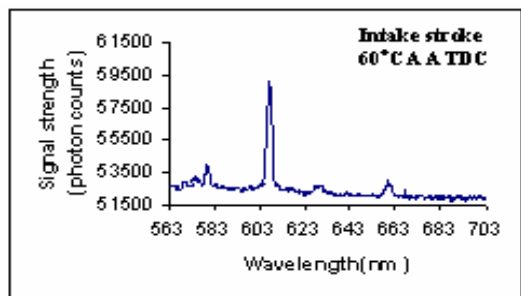
(b) SRS spectrum soon after the fresh charge first appeared

(e) SRS spectrum during the combustion

(c) SRS spectrum prior to the main combustion event

(f) SRS spectrum at the end of combustion

Figure 7 Sample SRS spectra during the mixture and combustion processes
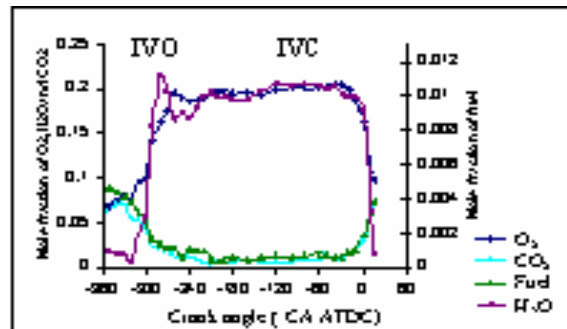
Figure 8 Mole fraction of H_2O, CO_2, O_2 and fuel at the centre of the combustion chamber, 3mm below the cylinder head

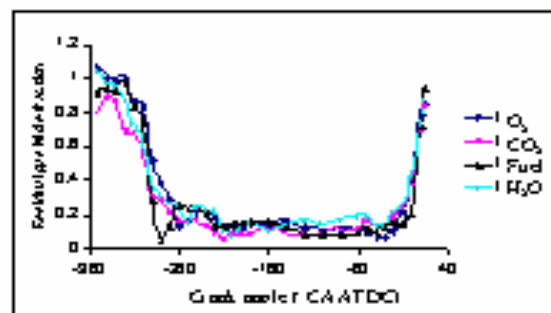**Figure 9** Mole fraction of residual gas calculated from the measured mole fraction of individual species
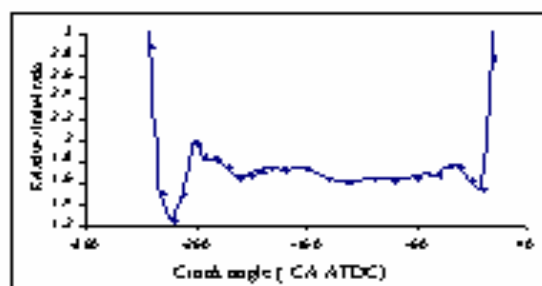

Figure 10 Relative air/fuel (λ value) ratio calculated from the measured mole fraction of O2 and fuel

Summary

   A SRS system for the simultaneous measurement of in-cylinder air/fuel ratio and residual gas concentration is described.

Mean mole fractions of O_2, N_2, H_2O, CO_2 and fuel in a CAI combustion engine during the mixture process and combustion process as a function of crank angle are presented.

Residual gas mole fractions are estimated from the individual species mole fractions. Air/fuel ratio is obtained from the measured mole fractions of fuel and O_2. It demonstrated that the SRS could provide simultaneous measurements of air/fuel ratio and residual gas concentration.

The measurement result during the combustion process shows that the SRS can provide valuable information on the auto-ignition and the chemical reaction process in a CAI combustion engine.

References:
1. Zhao, H., Peng, Z., Williams, J., Ladommatos, N., SAE Paper No. 2001-01-3607 (2001)
2. Mattias Richter, Axel Franke, J. Engstrom, A. Hultqvist, Bengt Johansson, SAE Paper No. 2000-01-2 (2000)
3. Johnston, S.C.*, SAE Paper No. 790433 (1979)
4. Johnston, S.C., SAE Paper No. 800136 (1980)
5. Grunefeld, G. and Beushausen, V., SAE Paper No. 941880 (1994)
6. Grunefeld, G., Knapp, M., Beushausen, V., Andresen, P., Hentschel, W. and Manz, P*, SAE Paper No. 952394 (1995)
7. Knapp, M., Beushausen, V., Hentschel, W., Manz, P., Grunefeld, G. and Andresen, SAE Paper No. 970827 (1997)
8. Schutte, M., Finke, H., Grunefeld, G., Kruger, S., Andresen, P., Stiebels, B., Block, B., Meyer, H. and Hentschel, W., SAE Paper No. 2000-01-1795 (2000)
9. Miles, P. and Dilligan, M., SAE Paper No. 960828 (1996)
10. Miles, P.C. and Hinze, P.C., SAE Paper No. 981428 (1998)
11. Hinze, P.C. and Miles, P.C., *, SAE Paper No. 1999-01-1106 (1999)